Published in final edited form as:
Mol Cancer Res. 2012 February ; 10(2): 218–229. doi:10.1158/1541-7786.MCR-11-0451.

Caveolin-1 Upregulation Contributes to c-Myc–Induced High-Grade Prostatic Intraepithelial Neoplasia and Prostate Cancer

Guang Yang[1], **Alexei A. Goltsov**[1], **Chengzhen Ren**[1], **Shinji Kurosaka**[1], **Kohei Edamura**[1], **Richard Logothetis**[1], **Francesco J. DeMayo**[2], **Patricia Troncoso**[3], **Jorge Blando**[4,5], **John DiGiovanni**[4,5], and **Timothy C. Thompson**[1]

[1]Department of Genitourinary Medical Oncology – Research, The University of Texas MD Anderson Cancer Center, Houston, Texas

[2]Department of Molecular and Cellular Biology, Baylor College of Medicine, Houston Texas

[3]Department of Pathology, The University of Texas MD Anderson Cancer Center, Houston, Texas

[4]Department of Molecular Carcinogenesis, The University of Texas MD Anderson Cancer Center, Houston, Texas

[5]Department of Pharmacology, The University of Texas – Austin, Austin, Texas

Abstract

Previously we reported caveolin-1 (Cav-1) overexpression in prostate cancer (PCa) cells and demonstrated that it promotes PCa progression. Here, we report that Cav-1 was overexpressed in 41.7% (15 of 36) of high-grade prostatic intraepithelial neoplasia (HGPIN) specimens obtained during radical prostatectomies. Positive correlations exist between Cav-1–positive (Cav-1$^+$) HGPIN and Cav-1$^+$ primary PCa (rho = 0.655, $P < 0.0001$) and between Cav-1 and c-Myc expression in HGPIN (rho = 0.41, $P = 0.032$). To determine whether Cav-1 cooperates with c-Myc in development of premalignant lesions and PCa *in vivo*, we generated transgenic mice with c-Myc overexpression driven by the ARR_2PB promoter. In this ARR_2PB–c-myc model, Cav-1 overexpression was found in mouse PIN (mPIN) lesions and PCa cells and was associated with a significantly higher ratio of proliferative to apoptotic labeling in mPIN lesions than in the Cav-1–negative epithelia adjacent to those lesions (10.02 *vs* 4.34; $P = 0.007$). Cav-1 overexpression was also associated with increased levels of P-Akt and VEGF-A, which were previously associated with Cav-1–induced PCa cell survival and positive-feedback regulation of cellular Cav-1 levels, respectively. In multiple PCa cell lines, Cav-1 protein (but not mRNA) was induced by c-Myc transfection, whereas VEGF siRNA transfection abrogated c-Myc–induced Cav-1 overexpression, suggesting a c-Myc–VEGF–Cav-1 signaling axis. Overall, our results suggest that Cav-1 is associated with c-Myc in the development of HGPIN and PCa. Further, Cav-1 overexpression in HGPIN is potentially a biomarker for early identification of patients who tend to develop Cav-1$^+$ primary PCa.

Keywords

Caveolin-1; c-Myc; prostatic intraepithelial neoplasia; prostate cancer; metaplasia

Corresponding Author: Timothy C. Thompson, Department of Genitourinary Medical Oncology – Research, Unit 18-3, The University of Texas MD Anderson Cancer Center, 1515 Holcombe Boulevard, Houston, TX 77030-4009. Phone: 713-792-9955; Fax: 713-792-9956; timthomp@mdanderson.org.

Disclosure of Potential Conflicts of Interest: The authors declare no potential conflicts of interest.

Introduction

A dilemma facing urologic oncologists today is whether all patients with prostate cancer (PCa) who are aggressively treated with radical prostatectomy actually benefit from that invasive therapy. As many as 16% of radical prostatectomy specimens contain only small, well-differentiated cancers that may never achieve clinical significance during the patient's lifetime (1, 2), whereas more than 50% of cancers considered preoperatively to be localized to the prostate are subsequently found extraprostatically and thus have a high risk of progression (3). Some preoperative indices, including prostate-specific antigen concentration and Gleason score of the carcinoma specimen obtained on needle biopsy, are important predictors of pathologic and clinical outcome. However, their predictive power is greatly diminished for cancers in the middle range of a given index. Thus, molecular markers that may supplement clinical information and predict cancer progression potential at an early stage of malignancy are being actively sought.

Caveolin-1 (Cav-1), a 22-kD structural protein of the caveolae, specialized invaginations in the plasma membrane, is an important mediator of molecular transport, cell adhesion, and cell signaling (4). The role of Cav-1 in tumorigenesis is complex, depending on cell type and biologic context. Under some conditions, Cav-1 may suppress tumorigenesis (5), although Cav-1 upregulation is also associated with and contributes to the progression of multiple malignancies, including PCa (6). PBcav-1 transgenic mice, which have targeted overexpression of Cav-1 in their prostatic epithelial cells, demonstrate prostatic hyperplasia (7), and in the TRAMP (transgenic adenocarcinoma mouse prostate) PCa model, loss of Cav-1 function leads to fewer primary tumors and metastatic lesions (8). In addition, suppression of Cav-1 expression with stably transfected antisense Cav-1 cDNA converts androgen-insensitive metastatic mouse PCa cells to an androgen-sensitive phenotype (9). Moreover, an immunohistochemical study of 162 clinically confined human PCa specimens obtained from radical prostatectomies demonstrated that Cav-1 expression is a novel independent prognostic biomarker for recurrence after prostatectomy (10).

Mechanistic studies have revealed that Cav-1 contributes to PCa progression by activating PI3-K–Akt signaling and Akt target genes involved in inhibiting apoptosis in metastatic PCa cells (11). Cav-1 expression also generates autocrine and paracrine positive-feedback loops by increasing VEGF (vascular endothelial growth factor), TGF-β1 (transforming growth factor beta 1), and FGF2 (fibroblast growth factor 2)mRNA stability, leading to increased levels of these proteins and increased invasiveness of PCa cells (12) and proangiogenic activities (13). Cav-1 expression can also elevate cellular fatty acid synthase levels (14) and potentiate ligand-dependent androgen receptor activation (15).

Abnormal regulation of the c-Myc oncogene has been documented extensively in PCa. Its amplification in metastatic and/or hormone-refractory PCa was reported previously. More recent studies have documented amplification of the *c-MYC* locus on chromosome 8q24 in a subset of aggressive PCas (16). Results of other recent studies point to an essential role for c-Myc in oncogenic transformation of prostate epithelia. For example, nuclear c-Myc overexpression is found in high-grade prostatic intraepithelial neoplasia (HGPIN), the premalignant stage of human PCa (17). Additionally, introduction of the wild-type c-Myc has been reported to be sufficient to cause primary prostate epithelial cells to develop cancer phenotypes *in vitro* and in a tissue recombination model (18). In the C(3)1–*c-myc* transgenic mouse model, enforced prostate epithelial cell–specific c-Myc expression induces formation of PIN lesions (19). Finally, transgenic c-Myc expression under the transcriptional regulation of the rat probasin (PB) promoter can result in the development of mouse PIN (mPIN) and invasive adenocarcinoma (20). Further, transduction of the *v-Myc* oncogene results in epithelial hyperplasia, and *v-Myc* cooperates with the *ras* oncogene to generate

PCa in the mouse prostate reconstitution model (21). The findings that c-Myc activation by protein kinase Cε, a protein overexpressed in most advanced PCas, may drive downstream Cav-1 overexpression in hormone-independent CWR-R1 cells (22) and that Cav-1 overexpression in LNCaP PCa cells may inhibit c-Myc–induced apoptosis (23) suggest that Cav-1 is functionally associated with c-Myc. Our previous results demonstrating that Cav-1 overexpression correlates positively with c-Myc overexpression in clinically confined human PCas (24) also support this thought.

Because Cav-1 and c-Myc expression are closely associated in human PCa (23, 24), we hypothesized that Cav-1 is associated with and contributes to c-Myc–induced HGPIN and PCa. To test this hypothesis, we immunohistochemically analyzed human prostate specimens containing HGPIN lesions to identify any associations between Cav-1 and c-Myc expression in these lesions. First we used specimens in which HGPIN coexisted with PCa (adenocarcinoma) so we could identify any association between Cav-1 expression in HGPIN and in PCa. Then, to further investigate any relationship between Cav-1 and c-Myc expression in PIN and the transition to PCa, we generated and characterized a new mouse transgenic model in which enforced prostate-specific c-Myc overexpression is driven by the ARR_2PB promoter (25). In this model, c-Myc overexpression leads predominantly to development of mPIN, which is morphologically similar to human HGPIN, and microinvasive adenocarcinoma develops at a low frequency.

By using specimens in which HGPIN coexists with PCa and our new transgenic mouse model, we demonstrated and then confirmed the existence of a positive association between c-Myc overexpression and Cav-1 upregulation in mPIN and PCa cells. Our results further suggest a role for c-Myc–VEGF–Cav-1 signaling in the development of PCa.

Materials and Methods

Human prostate specimens

We used prostate specimens that had been obtained previously during radical prostatectomies with the approval of our institutional review board and written informed consent from the patients. The formalin-fixed, paraffin-embedded specimens were archived in the Tissue Core facility funded by the prostate Specialized Program of Research Excellence (SPORE P50-CA140388) grant at The University of Texas MD Anderson Cancer Center. For pathologic evaluation, 5 μm–thick cross sections of the tissues were stained with hematoxylin and eosin, and an experienced pathologist (P.T.) identified for our study specimens that contained HGPIN lesions coexisting with at least 1 adenocarcinoma focus. Because of this criterion, we could use the specimens not only for identifying any association between Cav-1 and c-Myc expression in HGPIN but also for analyzing the relationship between Cav-1 expression in HGPIN and that in PCa after Cav-1 and c-Myc immunostaining (Fig. 1).

Generation of ARR_2PB–c-myc transgenic mice

C57BL/6J mice were used to generate ARR_2PB-c-myc transgenic mice; the mice were maintained in facilities accredited by the American Association for Accreditation of Laboratory Animal Care. All procedures involving animals were approved by the Institutional Animal Care and Use Committee of the Univeristy of Texas MD Anderson Cancer Center.

To target expression of the human c-Myc transgene to the mouse prostate epithelium, we expressed c-Myc cDNA under control of the ARR_2PB promoter, in which the rat PB promoter was modified by inserting a sequence composed of 2 repeats of the androgen-responsive region (i.e., ARR_2) (25). The transgenic construct is depicted in Figure 2. The

400-bp *XbaI-BamI* DNA fragment containing theARR_2PB promoter was excised from the pXCJL-1–ARR_2PB–polyA vector (kindly provided by Dr. M. Marcelli, Baylor College of Medicine, Houston, TX) and used to replace the MMTV promoter in the pMMTV–KCR–bovine growth hormone polyA (bGHpA) vector (26). To maximize expression of the transgene, we added the rabbit β-globin gene fragment KCR, which comprises exon II, intron II, exon III, and poly(A) signal sequences derived from the rabbit β-globin gene and contains the requisite splice donors and acceptors. The 1.8-kb EcoRI fragment containing full-length human c-Myc cDNA was excised from the pSP–c-Myc vector (a generous gift from Dr. R.N. Eisenman, Fred Hutchinson Cancer Center, Seattle, WA) and inserted into the EcoRI site of the pARR_2PB–KCR–bGHpA vector.

The resulting Sal-I DNA fragment containing the ARR_2PB–KCR–c-Myc–bGHpA transgene devoid of vector sequences was gel purified. The purified transgene DNA was then microinjected into the pronucleus of a fertilized C57BL/6J mouse embryos that were then transplanted into the uteri of pseudopregnant C57BL/6female according to the standard technique used in the Transgenic Core facility at Baylor College of Medicine. The resulting transgenic offspring were screened by performing polymerase chain reaction (PCR) analysis on genomic DNA isolated from tail snips. The forward primer was specific to the 5′ end of the KCR sequence (5′GGATCCTGAGAACTTCAG3′), and the reverse was located at the c-myc cDNA (5′GTAGAAATACGGCTGCAC3′).

Four founder lines (32T, 35T, 37T, and 39T) were generated and, after breeding, germline transmission was confirmed. Mice were euthanized when they were 3 to 17 months old, and ventral, anterior, and dorsolateral prostates were obtained from the male transgenic mice and their wild-type littermates. In addition, liver, kidney, seminal vesicle, small intestine, spleen, lung, brain, and heart tissues were obtained. Part of each tissue was fixed in 10% phosphate-buffered formalin (0.01 M, pH 7.4) for 3 hours and then embedded in paraffin and cut into 5-μm sections for hematoxylin and eosin staining or immunostaining; another part was frozen in liquid nitrogen and processed for RNA and protein analysis. Initial quantitative reverse-transcription (qRT)-PCR analysis of *c*-myc transgene expression in the multiple organs was performed on RNA by using the TaqMan protocol (Invitrogen, Carlsbad, CA) customized for the ARR_2PB–KCR–c-Myc–bGHpA transgene.

We also used paraffin-embedded sections of several prostates obtained from Hi-Myc transgenic mice developed originally by Ellwood-Yen and coworkers (20) for Cav-1 immunostaining.

Immunohistochemical analyses of prostate tissues

Autibodies to Cav-1, VEGF-A (Santa Cruz Biotechnology, Santa Cruz, CA), c-Myc (clone Y79, Epitomics, Inc., Burlingame, CA), PCNA and P-Akt (pSer473,, Cell Signaling Technology, Inc., Danvers, MA) were used for immunostaining on formalin-fixed paraffin-embedded tissues from both the mouse and human prostate specimens. All tissue sections were processed by using an avidin-biotin peroxidase complex kit (ABC; Vector Laboratories, Burlingame, CA). Detailed descriptions of staining procedures for each antibody are described in Supplemental Methodology.

Apoptotic-body labeling by TUNEL technique

The TUNEL (terminal deoxynucleotidyl transferase-mediated dUTP-biotin nick-end labeling) technique was used to label apoptotic bodies on mouse prostate tissue slides with a TUNEL cell death–detection kit (Millipore, Billerica, MA), following the manufacturer's recommended procedure.

Quantitation of immunohistochemical labeling

Because of the heterogeneity of Cav-1 expression, a specimen was considered to have Cav-1–positive (Cav-1^+) HGPIN when it had more than 1 glandular HGPIN profile in which more than 50% of the neoplastic epithelial cells stained positively for Cav-1. PCa specimens were considered Cav-1^+ if they met the previously established criteria (10).

For quantitation of c-Myc immunostaining, multiple RGB images from HGPIN or PCa areas were acquired by using an image-analysis system equipped with a motorized stage (Eclipse 90i; Nikon Instruments, Inc., Melville, NY). Images were analyzed at 200× by using Nikon's NIS-Elements version 3.0 software. The areas of HGPIN and PCa on each image (i.e., the region of interest) were outlined manually, and all stromal areas and nontargeted epithelia were excluded.

The blue nuclear hematoxylin staining in the areas of HGPIN and PCa was identified and recorded by using a pixel classifier that assesses color intensity, saturation, and hue on images. The total area of brown immunostaining of c-Myc in the epithelial cells of HGPIN and PCa was measured and recorded by using another pixel classifier that recognizes only nuclear DAB staining. The ratio of the area of nuclear DAB staining to the total nuclear area (defined as the sum of the DAB- and hematoxylin-stained areas) was measured separately within HGPIN and cancerous epithelial compartments. This ratio, known as the nuclear c-Myc ratio, is positively correlated with the c-Myc^+ nuclear fraction and has been used successfully for evaluating the nuclear expression of c-Myc in human prostates (17). For each specimen, we also acquired 10 images of histologically normal luminal epithelia from regions at least 10 mm away from a neoplasm; those images were analyzed by using the same technique just described.

To quantitate the immunostaining for PCNA and apoptotic bodies in the prostates from the transgenic mice, 10 to 20 microscopic fields (400×) were evaluated for each specimen. The numbers of $PCNA^+$ cells and apoptotic bodies were counted and recorded as PCNA and apoptotic-body labeling rates (%).

Cell lines and transfections

All human PCa cell lines used in our experiments were validated by STR DNA fingerprinting using the AmpFℓSTR® Identifier kit (Applied Biosystems) in the MD Anderson Cancer Center Cell Line Core. The cell lines were grown in the following media: VCaP, in high-glucose DMEM with 10% FBS; LNCaP and PC-3, in RPMI 1640 with 10% FBS; and LAPC-4, in IMDM with 15% FBS. Cells were grown in 6-well plates and transfected with pcdna3.1–c-Myc plasmid or with empty pcdna3.1 vector by using Fugene HD (Roche) transfection reagent. In some experiments, PC-3 cells were also transfected with VEGF-specific small interfering RNA (siRNA; Ambion–Invitrogen or Santa Cruz Biotechnology, Santa Cruz, CA) by using Lipofectamine RNAiMax (Invitrogen) 24 hours before being transfected with pcdna3.1–c-myc or empty pcdna3.1 vector.

Immunoblotting

Cultured cells from human PCa cell lines were collected 24, 48, and 72 hours after transfection, and expression of specific proteins was analyzed by immunobloting as described previously (12) with a mouse monoclonal (BD Biosciences, Pasadena, CA) or a rabbit polyclonal (Santa Cruz) Cav-1 antibody; with a rabbit polyclonal VEGF-A antibody (Santa Cruz); and with a rabbit monoclonal c-Myc antibody (Epitomics). A β-actin monoclonal antibody (Sigma-Aldrich) was used as the loading control.

Statistical analysis

The correlations between (a) Cav-1 immunostaining in HGPIN and that in PCa and (b) Cav-1 immunostaining with c-Myc immunolabeling in HGPIN and that in adenocarcinomas were analyzed by using Spearman's rank-order correlation coefficient (rho [ρ]) or Fisher's exact testing. The Kruskal-Wallis test was used to analyze the relationships between nuclear c-Myc ratio and either the Gleason score or the pathologic stage of the PCas. The nuclear c-Myc ratios in normal epithelial, HGPIN, and PCa compartments were compared by using Mann-Whitney testing. ANOVA analysis followed by Student's *t* testing was used to compare the PCNA labeling rates, apoptotic-body labeling rates, and proliferation-to-apoptosis ratios between the normal epithelia and the mPIN lesions in the transgenic mice and between the normal epithelia of the transgenic mice and that of the wild-type mice. All analyses were performed with Statview statistical software (version 5.0; SPSS Inc., Chicago, IL). *P* values < 0.05 were considered statistically significant in all analyses.

Results

Cav-1 overexpression in HGPIN in human radical prostatectomy specimens

Thirty-six archived prostate specimens met our criteria and were included in this study. Thirty-one of the specimens (86%) were pathologic stage pT2, 4 were pT3a, and 1 was pT3b. Sixteen of the specimens had a Gleason score 6; 17, a score 7; 2, a score 8; and 1, a score 9.

In the histologically normal regions of the 36 specimens, Cav-1^+ immunostaining was abundant in the stromal and vascular cells, whereas it was almost undetectable in the prostate luminal epithelial cells (Figure 1). In contrast, in the stromal cells of some Cav-1^+ HGPINs or PCas, the level of immunostaining tended to be lower than it was in the stroma surrounding the normal glandular epithelia. Further, Cav-1^+ immunostaining was detected in the glandular epithelia of HGPIN regions and in the cancer foci in some specimens, usually in a focal distribution pattern. Fifteen (41.7%) of the 36 specimens had Cav-1^+ HGPIN, and these specimens also tended to have Cav-1^+ cancer (Table 1); this correlation was statistically significant ($\rho = 0.655$; $P < 0.001$, Fisher's exact test).

Among the 36 specimens used for Cav-1 immunostaining, 31 (86%) also had tissue slides available for c-Myc immunostaining. c-Myc^+ staining was most abundant in the nuclei of the HGPIN and cancer cells, although some weaker labeling was observed in the cytoplasm as well (Figure 1, *E* and *F*). In this cohort of 31 specimens, the mean nuclear c-Myc ratios determined on image analysis were 0.111 in the prostate epithelia as a whole, 0.022 in the normal epithelia, 0.125 in the HGPIN areas, and 0.184 in the PCa compartment. The median nuclear c-Myc ratios in the HGPIN (0.086; range, 0.003–0.547) and PCa (0.068; range, 0.003–0.784) compartments were significantly higher than the ratio in the normal glandular epithelia (0.022; range, 0.004–0.066) ($P < 0.001$ for both comparisons, Mann-Whitney test), suggesting that c-Myc is overexpressed in these lesions relative to its expression in normal glandular epithelia (Figure 1).

The nuclear c-Myc ratio in the cancer compartment did not correlate with either the Gleason score or the pathologic stage of the PCa in this cohort ($P = 0.236$ and $P = 0.359$, respectively, Kruskal-Wallis test).

When the nuclear c-Myc ratios in the HGPIN or cancer compartment were stratified according to Cav-1 expression status (Figure 1), the median ratio in the Cav-1^+ HGPIN (0.161; range, 0.027–0.547) was significantly higher than that in the Cav-1–negative (Cav-1^-) HGPIN (0.052; range, 0.003–0.442; $P = 0.021$, Mann-Whitney test). The median

nuclear c-Myc ratio was also significantly higher in the Cav-1$^+$ cancers (0.360; range, 0.005–0.784) than it was in the Cav-1$^-$ cancers (0.037; range, 0.003–0.435; $P = 0.0039$).

To further analyze the correlation between Cav-1 and c-Myc expression, we used the overall mean nuclear c-Myc ratio (0.11) as the cutoff value to stratify those ratios (Table 1) in this set of 31 specimens immunostained with both Cav-1 and c-Myc. At this cutoff level, 10 of 14 (71.4%) Cav-1$^+$ HGPINs had a nuclear c-Myc ratio greater than 0.11 and were categorized as c-Myc$^+$, whereas 5 of 17 (29.4%) of Cav-1$^-$ HGPINs were c-Myc$^+$. This difference was statistically significant ($P = 0.032$, Fisher's exact test). Among the 12 Cav-1$^+$ cancer specimens, 10 (83.3%) were c-Myc$^+$, compared with only 3 (15.8%) of the 19 Cav-1$^-$ cancers that were c-Myc$^+$ ($P< 0.001$, Fisher's exact test).

Characterization of ARR$_2$PB–c-myc transgenic mice

To further investigate the correlations between increased c-Myc expression and Cav-1 positivity in the human HGPIN specimens, we generated the ARR$_2$PB–c-myc transgenic mouse model. We verified the transgenic c-Myc expression by performing Western blotting with protein extracts of the prostates both from the transgenic mice that had been positively genotyped and from wild-type mice using a rabbit monoclonal antibody specific to c-Myc. A high level of c-Myc protein was found in the ARR$_2$PB–c-myc transgenic but not in the wild-type prostates (Figure 2B), confirming expression of the c-Myc transgene.

We further verified the transgenic c-Myc expression using immunostaining. c-Myc expression was not detected in any prostate lobe of the wild-type mice. In contrast, c-Myc$^+$ staining was predominantly nuclear in the neoplastic glandular epithelia of the ARR$_2$PB–c-myc transgenic prostates; weaker cytoplasmic staining was apparent in these cells. Regional differences in c-Myc expression were found in the transgenic prostates: it was broadly induced in the glandular epithelia of the dorsolateral and ventral prostate lobes but was confined to some glandular segments of the anterior lobe (Figure 2C).

c-Myc transgene expression leads to formation of mPIN lesions, microinvasive adenocarcinomas, and metaplasia

The hematoxylin- and eosin-stained sections of prostate tissues from the ARR$_2$PB–c-myc transgenic mice were evaluated histologically according to the previously established criteria for transgenic mice(27). The glandular epithelia in all prostate lobes of the ARR$_2$PB–c-myc transgenic mice (n=41) had morphologic characteristics that differed from those in the wild-type counterparts (n=26) (Figure 2D). The changes, which included epithelial thickening, tufting, and cribriform formation; enlarged cell size and nuclei with prominent nucleoli; and increased numbers of mitotic and apoptotic figures, all indicated formation of mPIN. We also observed that the most severe mPIN lesions were in the dorsal lobe, where cribriform glands had become the major structural form. The anterior lobes exhibited mainly focal mPIN lesions in which there were only a few granular profiles or only part of a gland was involved. Microinvasive carcinoma cells were seen sprouting out of the mPIN lesions and forming small nests or masses of neoplastic cells in the periglandular stroma.

The incidence rates of mPIN lesions and carcinomas increased with age (Table 2).

Further, mucinous metaplasia was observed in different prostatic lobes of the ARR$_2$PB–c-myc mice (Figure 2D). These cells resided adjacent to the neoplastic lesions and featured the presence of a mucin-like substance in the cytoplasm and basally localized nuclei.

Cav-1 overexpression in the prostatic epithelia of the ARR_2PB–c-myc mice is specifically localized to the mPIN lesions and microinvasive adenocarcinomas

To determine whether enforced expression of the c-Myc transgene leads to Cav-1 expression in prostatic glandular epithelia, we performed immunostaining. As Figure 3 illustrates, Cav-1 was undetectable in the normal luminal epithelial cells in the prostates of the wild-type mice; immunostaining was confined to the stromal compartment, where multiple layers of periglandular myofibroblasts and vascular endothelial cells were strongly Cav-1^+. In sharp contrast, the prostatic glandular epithelia in the transgenic mice were Cav-1^+: high Cav-1 levels were observed in the mPIN lesions in mice as young as 3 months old. Further, there was an evident difference in Cav-1 expression by lobe in the transgenic mice. Cav-1 was almost universally present throughout the epithelia of the dorsolateral and ventral lobes, whereas in the anterior lobe, Cav-1^+ staining was confined to the regions that were also c-Myc^+.

The cells of the microinvasive adenocarcinomas in the transgenic mice were also strongly Cav-1+ (Figure 3). Additionally, the Cav-1 levels in the stromal myofibroblasts that surround the glandular epithelia were remarkably lower in the transgenic mice than they were in the wild-type mice.

Of note, Cav-1 expression was also observed in the glandular epithelia of mPIN lesions and invasive adenocarcinomas in the Hi-Myc transgenic mice.

Cav-1 overexpression in mPIN lesions is associated with a relative reduction of apoptosis and upregulation of P-Akt and VEGF

The proliferative and apoptotic activities in the epithelia of the anterior prostate lobes were examined by using PCNA immunostaining and TUNEL techniques, respectively. Quantitative image analysis allowed parallel comparisons of PCNA and apoptotic-body labeling rates between Cav-1^+ mPIN lesions and the Cav-1^- epithelia adjacent to those lesions in the same transgenic mice (Figure 4A). The numbers of $PCNA^+$ cells and apoptotic bodies were relatively greater in Cav-1^+ mPIN and microinvasive adenocarcinomas (data not shown), confirming that the c-Myc transgene induces proliferative and apoptotic activities.

The mPIN lesions in the transgenic mice had a 74.16% PCNA labeling rate, which is 37 times higher than that in the normal glands adjacent to the lesions (2.03%; $P< 0.0001$). Further, the PCNA labeling rate in the normal glands adjacent to the mPIN lesions in the transgenic mice was significantly higher than that in the normal epithelia of the wild-type mice ($P = 0.0267$).

In the mPIN lesions, the 8% labeling rate of apoptotic bodies was 12.5 times higher than it was in the adjacent normal epithelia (0.64%; $P< 0.0001$). The difference between the apoptotic-body labeling rates in the normal epithelia adjacent to mPIN lesions and in the wild-type epithelia was not statistically significant ($P = 0.491$).

When we compared the ratios between the PCNA and apoptotic-body labeling rates, it was interesting that the ratio in the mPIN lesions (10.02) was significantly higher than it was in the normal epithelia adjacent to the mPIN lesions in the transgenic mice (4.34) and in the wild-type epithelia (3.08; $P = 0.0001$ and $P = 0.0006$, respectively, for the two comparisons). Although the ratio was also higher in the normal epithelia adjacent to the mPIN lesions (4.34) than it was in the wild-type epithelia (3.08), that difference did not reach statistical significance ($P = 0.409$). The higher PCNA:apoptosis ratio indicates lower apoptotic activity relative to the drastically increased proliferative activity in the mPIN

lesions, compared with the activities in the epithelia adjacent to mPIN lesions in the transgenic mice.

Since our previous in vitro studies had identified an increased P-Akt level as a molecular event that contributes to Cav-1–induced PCa cell survival(11), we used immunostaining to compare P-Akt (S473) levels in the Cav-1^+ mPIN lesions and the Cav-1^- normal glandular epithelia adjacent to mPIN in the transgenic mice. We found P-Akt–positive immunostaining in the mPIN lesions and microinvasive carcinomas in the transgenic mice (Figure 4B), but positive staining was minimal in the normal glandular epithelial cells adjacent to mPIN or cancer lesions in the transgenic mice and in the normal glandular epithelial cells in the wild-type animals.

Because Cav-1 and specific oncogenic growth factors, including VEGF, FGF2, and TGF-β1, establish a positive-feedback loop in PCa cells (12), we immunohistochemically determined their levels in the ARR_2PB–c-myc mice so that we could identify any association between those levels and Cav-1 overexpression. In the transgenic mice, the mPIN and cancer cells did not have any increased levels of FGF2 and TGF-β1, compared with those in the adjacent normal epithelial cells (data not shown). In contrast, the mPIN lesions and microinvasive carcinomas were strongly labeled by the VEGF antibody (Figure 4B). The prostate glandular tissues adjacent to the mPIN lesions in both the transgenic and wild-type mice stained negatively for VEGF-A.

c-Myc induces Cav-1 expression in PCa cell lines, in part through upregulation of VEGF-A

To evaluate whether Cav-1 overexpression in prostate epithelial cells can be induced by c-Myc overexpression in vitro, we analyzed Cav-1 expression in multiple PCa lines after transfecting them with the control vector pcdna3.1 or the c-Myc expression vector pcdna-c-myc. Cell lines with a relatively low to moderate level of endogenous Cav-1—VCaP, LNCaP, and PC-3—demonstrated upregulated Cav-1 protein expression 24 and 48 hours after c-Myc transfection (Figure 5). In LAPC4 cells, however, which have a moderate level of endogenous Cav-1, no significant changes occurred. None of the tested cell lines exhibited any significant changes in Cav-1 RNA levels in either the presence or absence of c-Myc (data not shown), suggesting that a posttranscriptional mechanism is involved.

The induction of Cav-1 by c-Myc may be a multistep process that can be explained by the stability of Cav-1 RNA or protein that occurred in response to c-Myc–stimulated gene activities, including the production of growth factors. Because we found that the induction of VEGF-A correlated with the induction of Cav-1 in response to c-Myc in VCaP, LNCaP, and PC-3 cells, we hypothesized that c-Myc induction stimulates angiogenic activities and that production of VEGF-A may in turn stimulate Cav-1 expression. To test this hypothesis, we used VEGF siRNA (siVEGF) to knock down VEGF-A expression in PC-3 cells and followed that by transfecting them with pcdna3.1 vector or pcdna-c-myc. The results showed that siVEGF but not control siRNA (siNC) downregulates VEGF-A protein expression 72 hours after the initial VEGF siRNA transfection (Figure 5B: compare siNC and siVEGF). Transfection with c-myc induced Cav-1 expression as before (Figure 5B: compare siNC– and siNC+ c-myc). However, Cav-1 induction by c-Myc was reduced in VEGF-knockdown conditions (Figure 5B: compare siNC+ and siVEGF+ c-Myc.

Together, these results show that induction of Cav-1 expression in response to c-Myc may be at least partly mediated through c-Myc–stimulated VEGF expression (Figure 5C).

Discussion

Our finding that Cav-1 was expressed in 41.7% of the human HGPIN specimens we analyzed suggests that Cav-1 is involved in the development of premalignant lesions in a subgroup of PCa patients. We also found a positive association between Cav-1 and c-Myc immunostaining in both HGPIN and PCa. Further, our results revealed a highly significant association between Cav-1^+ HGPIN and Cav-1^+ PCa. Thus, our overall immunostaining results in human PCa samples suggest that Cav-1 and c-Myc cooperate in the development of HGPIN and in the transition from HGPIN to PCa. In a previous study, we demonstrated that patients who have Cav-1^+ PCas have a higher risk of developing metastasis and disease progression (28). This newly revealed association between Cav-1 overexpression in HGPIN and that in PCa further suggests that Cav-1^+ immunostaining in HGPIN may be useful as an early biomarker for identifying patients who will develop a Cav-1^+ cancer and therefore have a high risk of progression. It will be interesting to determine in a future study whether the presence of a Cav-1^+ HGPIN lesion in a prostate biopsy specimen has independent predictive value for the development and progression of PCa.

To further investigate the relationship we found between c-Myc expression and Cav-1 expression as well as their interaction during the development of premalignant lesions and PCa in vivo, we generated the new ARR_2PB–c-myc transgenic mouse model. Our new model bears similarities to the Hi-Myc model previously established by Ellwood-Yen and coworkers (20) in that both models use the ARR_2PB promoter to enforce transgenic c-Myc expression. However, some differences exist. First, our model contains the full-length 1.8-kb human c-*MYC* cDNA instead of a 1.3-kb sequence in which only the open reading frame was constructed in the transgene. Second, our new ARR_2PB–c-myc construct does not include the Flag-tagged sequences present in the Hi-Myc construct. The new ARR_2PB–c-myc construct was verified by sequencing. Third and finally, the new ARR_2PB–c-myc mice were generated using C57BL/6Jmice, whereas the Hi-Myc mice were generated using the FVB strain. In spite of these differences, our new transgenic mice, like the Hi-Myc mice, are characterized by the presence of mPIN lesions, which are morphologically similar to human HGPIN lesions and adenocarcinomas (27), although the frequency of adenocarcinomas in our new model was lower than that in the Hi-Myc model. It is interesting to note the presence of c-Myc-induced mucinous metaplasia in our model, which was not reported in the Hi-Myc model. In both animal models, our immunohistochemical analyses revealed increased Cav-1 immunostaining within all mPIN lesions and cancers but not in normal glandular epithelia; this finding does support a role for c-Myc overexpression in Cav-1 upregulation in these neoplastic lesions.

In a recent study, we demonstrated that transgenic Cav-1 overexpression in mouse prostate results in the generation of proliferative lesions characterized by epithelial hyperplasia with atypia (7). However, because the enforced Cav-1 expression in that study did not induce mPIN or adenocarcinoma, we concluded that overexpression of the *Cav-1* gene by itself is unable to directly induce oncogenic transformation; further, we concluded that Cav-1 may be involved in oncogenic transformation by mediating the expression and function of oncogenic growth factors (12). The new findings we report here of Cav-1 overexpression in ARR_2PB–c-myc mice provide the first in vivo evidence that in association with overexpression of c-Myc, Cav-1 overexpression is associated with the development of premalignant lesions and the transition to malignancy.

To investigate the role of Cav-1 in c-Myc–induced PIN and PCa, we compared the proliferative and apoptotic activities in the ARR_2PB–c-myc transgenic prostate epithelia between the Cav-1^- histologically normal glands and the Cav-1^+ mPIN lesions induced by the c-Myc transgene. Among the numerous functions c-Myc has as a proto-oncogene, its

cell-proliferative and apoptotic activities are 2 major context-dependent functions that are driven by its activation (29, 30). Relatively increased proliferative activity and inhibition of apoptosis elicited by deregulated c-Myc expression reportedly may lead to the development of malignancy (29, 31). In our ARR_2PB–c-myc transgenic mice, the significantly increased PCNA labeling rate in mPIN lesions was accompanied by a relatively small increase in apoptotic-body labeling rate, which resulted in a larger PCNA labeling:apoptotic-body labeling ratio in mPIN than that in adjacent normal prostatic epithelia, indicating relative inhibition of apoptosis in Cav-1^+ mPIN lesions.

In another previous study, we showed that inhibition of Cav-1 scaffolding domain–binding sites on PP1 and PP2A led to significantly increased levels of P-Akt and sustained activation of downstream oncogenic Akt targets that promote cell survival (11). Given those results, the co-overexpression of Cav-1 and P-Akt demonstrated by our new immunostaining results in the Cav-1^+ mPIN lesions of the ARR_2PB–c-myc mice strongly suggests a role for Cav-1 in Akt activation in this context. Further, it has been shown that Akt activation may inhibit c-Myc–induced apoptosis (32-34). We previously demonstrated that the Cav-1 upregulation by Cav-1 transfection of LNCaP cells suppressed c-Myc–induced apoptosis and facilitated the growth of cancer cell colonies in soft agar (23). Our new results, together with those of previous studies, suggest that Cav-1–mediated Akt activation contributes to c-Myc–induced mPIN and the transition from PIN to PCa.

The mechanisms underlying the Cav-1 overexpression in the new ARR_2PB–c-myc mouse model remain to be explored. In PCa cell lines, c-Myc transfection induces elevated levels of Cav-1 protein but not of Cav-1 mRNA, a finding consistent with the results of the sequence analysis of the Cav-1 promoter (35). This promoter does not reveal a canonical E-box, the potential DNA sequence targeted by c-Myc; therefore, Cav-1 is not likely a direct target of c-Myc. Cav-1 upregulation by c-Myc in the ARR_2PB–c-myc mice and in cancer cells may instead be mediated by other factors via a posttranscriptional mechanism(s). We previously showed that cellular Cav-1 levels can be regulated by multiple growth factors, including VEGF, in PCa cells and that an elevated Cav-1 level may, via a reciprocal positive-feedback mechanism, increase cell-associated and secreted VEGF levels by stabilizing VEGF mRNA (12). c-Myc activation is essential for VEGF production and angiogenesis during development and tumor progression (36) and has been reported to stimulate VEGF translation or to increase VEGF protein levels in several cells (37, 38). Our results showing elevated co-expression of VEGF and Cav-1 in the mPIN lesions of ARR_2PB–c-myc mice and in human specimens, together with those demonstrating that VEGF siRNA blocks c-Myc–stimulated Cav-1 expression, suggest that VEGF may mediate the interactions between c-Myc and Cav-1. Possibly, a c-Myc–VEGF–Cav-1 positive-feedback cycle plays a role in the development of PIN and the transition to PCa (Figure 5C).

In summary, through immunostaining analysis of human HGPIN and PCa samples and similar analyses performed using a new mouse model of the transition from PIN to PCa (ARR_2PB–c-myc mice), we have demonstrated the existence of a close association between Cav-1 overexpression and c-Myc expression in neoplastic prostatic growth. Further immunostaining results and direct gene-transfer studies in vitro showed that VEGF expression can mediate c-Myc–stimulated Cav-1 upregulation, suggesting the existence of a c-Myc–VEGF–Cav-1 positive-feedback cycle. Additional studies are warranted to determine the importance of our results in the development of HGPIN and the transition to PCa.

Supplementary Material

Refer to Web version on PubMed Central for supplementary material.

Acknowledgments

We thank Karen F. Phillips, ELS, for her expert editorial assistance.

Financial Support: This work was supported in part by the National Institutes of Health through MD Anderson's Cancer Center Support Grant (CA016672), through SPORE grants (P50-CA58204 and P50-CA140388), and through grants R01CA68814 (to T.C.T.) and R01CA50588 (to T.C.T.); and by the United States Department of Defense grant DAMD 17-98-1-8575 (to T.C.T.).

References

1. Epstein JI, Walsh PC, Carmichael M, Brendler CB. Pathologic and clinical findings to predict tumor extent of nonpalpable (stage T1c) prostate cancer. JAMA. 1994; 271:368–74. [PubMed: 7506797]
2. Partin AW, Yoo J, Carter HB, Pearson JD, Chan DW, Epstein JI, et al. The use of prostate specific antigen, clinical stage and Gleason score to predict pathological stage in men with localized prostate cancer. J Urol. 1993; 150:110–4. [PubMed: 7685418]
3. Partin AW, Kattan MW, Subong EN, Walsh PC, Wojno KJ, Oesterling JE, et al. Combination of prostate-specific antigen, clinical stage, and Gleason score to predict pathological stage of localized prostate cancer. A multi-institutional update. JAMA. 1997; 277:1445–51. [PubMed: 9145716]
4. Harder T, Simons K. Caveolae, DIGs, and the dynamics of sphingolipid-cholesterol microdomains. Curr Opin Cell Biol. 1997; 9:534–42. [PubMed: 9261060]
5. Williams TM, Lisanti MP. Caveolin-1 in oncogenic transformation, cancer, and metastasis. Am J Physiol Cell Physiol. 2005; 288:C494–506. [PubMed: 15692148]
6. Yang G, Truong LD, Timme TL, Ren C, Wheeler TM, Park SH, et al. Elevated expression of caveolin is associated with prostate and breast cancer. Clin Cancer Res. 1998; 4:1873–80. [PubMed: 9717814]
7. Watanabe M, Yang G, Cao G, Tahir SA, Naruishi K, Tabata K, et al. Functional analysis of secreted caveolin-1 in mouse models of prostate cancer progression. Mol Cancer Res. 2009; 7:1446–55. [PubMed: 19737975]
8. Williams TM, Hassan GS, Li J, Cohen AW, Medina F, Frank PG, et al. Caveolin-1 promotes tumor progression in an autochthonous mouse model of prostate cancer: genetic ablation of Cav-1 delays advanced prostate tumor development in tramp mice. J Biol Chem. 2005; 280:25134–45. [PubMed: 15802273]
9. Nasu Y, Timme TL, Yang G, Bangma CH, Li L, Ren C, et al. Suppression of caveolin expression induces androgen sensitivity in metastatic androgen-insensitive mouse prostate cancer cells. Nat Med. 1998; 4:1062–4. [PubMed: 9734401]
10. Yang G, Truong LD, Wheeler TM, Thompson TC. Caveolin-1 expression in clinically confined human prostate cancer: a novel prognostic marker. Cancer Res. 1999; 59:5719–23. [PubMed: 10582690]
11. Li L, Ren CH, Tahir SA, Ren C, Thompson TC. Caveolin-1 maintains activated Akt in prostate cancer cells through scaffolding domain binding site interactions with and inhibition of serine/threonine protein phosphatases PP1 and PP2A. Mol Cell Biol. 2003; 23:9389–404. [PubMed: 14645548]
12. Li L, Ren C, Yang G, Goltsov AA, Tabata K, Thompson TC. Caveolin-1 promotes autoregulatory, Akt-mediated induction of cancer-promoting growth factors in prostate cancer cells. Mol Cancer Res. 2009; 7:1781–91. [PubMed: 19903767]
13. Tahir SA, Yang G, Goltsov AA, Watanabe M, Tabata K, Addai J, et al. Tumor cell-secreted caveolin-1 has proangiogenic activities in prostate cancer. Cancer Res. 2008; 68:731–9. [PubMed: 18245473]
14. Di Vizio D, Sotgia F, Williams TM, Hassan GS, Capozza F, Frank PG, et al. Caveolin-1 is required for the upregulation of fatty acid synthase (FASN), a tumor promoter, during prostate cancer progression. Cancer Biol Ther. 2007; 6:1263–8. [PubMed: 17786030]
15. Lu ML, Schneider MC, Zheng Y, Zhang X, Richie JP. Caveolin-1 interacts with androgen receptor. A positive modulator of androgen receptor mediated transactivation. J Biol Chem. 2001; 276:13442–51. [PubMed: 11278309]

16. Taylor BS, Schultz N, Hieronymus H, Gopalan A, Xiao Y, Carver BS, et al. Integrative genomic profiling of human prostate cancer. Cancer Cell. 2010; 18:11–22. [PubMed: 20579941]
17. Gurel B, Iwata T, Koh CM, Jenkins RB, Lan F, Van Dang C, et al. Nuclear MYC protein overexpression is an early alteration in human prostate carcinogenesis. Mod Pathol. 2008; 21:1156–67. [PubMed: 18567993]
18. Williams K, Fernandez S, Stien X, Ishii K, Love HD, Lau YF, et al. Unopposed c-MYC expression in benign prostatic epithelium causes a cancer phenotype. Prostate. 2005; 63:369–84. [PubMed: 15937962]
19. Zhang X, Lee C, Ng PY, Rubin M, Shabsigh A, Buttyan R. Prostatic neoplasia in transgenic mice with prostate-directed overexpression of the c-myc oncoprotein. Prostate. 2000; 43:278–85. [PubMed: 10861747]
20. Ellwood-Yen K, Graeber TG, Wongvipat J, Iruela-Arispe ML, Zhang J, Matusik R, et al. Myc-driven murine prostate cancer shares molecular features with human prostate tumors. Cancer Cell. 2003; 4:223–38. [PubMed: 14522256]
21. Thompson TC, Southgate J, Kitchener G, Land H. Multistage carcinogenesis induced by ras and myc oncogenes in a reconstituted organ. Cell. 1989; 56:917–30. [PubMed: 2538247]
22. Wu D, Terrian DM. Regulation of caveolin-1 expression and secretion by a protein kinase cepsilon signaling pathway in human prostate cancer cells. J Biol Chem. 2002; 277:40449–55. [PubMed: 12185081]
23. Timme TL, Goltsov A, Tahir S, Li L, Wang J, Ren C, et al. Caveolin-1 is regulated by c-myc and suppresses c-myc-induced apoptosis. Oncogene. 2000; 19:3256–65. [PubMed: 10918582]
24. Yang G, Timme TL, Frolov A, Wheeler TM, Thompson TC. Combined c-Myc and caveolin-1 expression in human prostate carcinoma predicts prostate carcinoma progression. Cancer. 2005; 103:1186–94. [PubMed: 15712208]
25. Zhang J, Thomas TZ, Kasper S, Matusik RJ. A small composite probasin promoter confers high levels of prostate-specific gene expression through regulation by androgens and glucocorticoids in vitro and in vivo. Endocrinology. 2000; 141:4698–710. [PubMed: 11108285]
26. Ma ZQ, Chua SS, DeMayo FJ, Tsai SY. Induction of mammary gland hyperplasia in transgenic mice over-expressing human Cdc25B. Oncogene. 1999; 18:4564–76. [PubMed: 10467401]
27. Shappell SB, Thomas GV, Roberts RL, Herbert R, Ittmann MM, Rubin MA, et al. Prostate pathology of genetically engineered mice: definitions and classification. The consensus report from the Bar Harbor meeting of the Mouse Models of Human Cancer Consortium Prostate Pathology Committee. Cancer Res. 2004; 64:2270–305. [PubMed: 15026373]
28. Tahir SA, Frolov A, Hayes TG, Mims MP, Miles BJ, Lerner SP, et al. Preoperative serum caveolin-1 as a prognostic marker for recurrence in a radical prostatectomy cohort. Clin Cancer Res. 2006; 12:4872–5. [PubMed: 16914574]
29. Dang CV. c-Myc target genes involved in cell growth, apoptosis, and metabolism. Mol Cell Biol. 1999; 19:1–11. [PubMed: 9858526]
30. Evan G, Littlewood T. A matter of life and cell death. Science. 1998; 281:1317–22. [PubMed: 9721090]
31. Dang CV, Resar LM, Emison E, Kim S, Li Q, Prescott JE, et al. Function of the c-Myc oncogenic transcription factor. Exp Cell Res. 1999; 253:63–77. [PubMed: 10579912]
32. Kauffmann-Zeh A, Rodriguez-Viciana P, Ulrich E, Gilbert C, Coffer P, Downward J, et al. Suppression of c-Myc-induced apoptosis by Ras signalling through PI(3)K and PKB. Nature. 1997; 385:544–8. [PubMed: 9020362]
33. Rohn JL, Hueber AO, McCarthy NJ, Lyon D, Navarro P, Burgering BM, et al. The opposing roles of the Akt and c-Myc signalling pathways in survival from CD95-mediated apoptosis. Oncogene. 1998; 17:2811–8. [PubMed: 9879987]
34. Ramljak D, Coticchia CM, Nishanian TG, Saji M, Ringel MD, Conzen SD, et al. Epidermal growth factor inhibition of c-Myc-mediated apoptosis through Akt and Erk involves Bcl-xL upregulation in mammary epithelial cells. Exp Cell Res. 2003; 287:397–410. [PubMed: 12837294]
35. Bist A, Fielding PE, Fielding CJ. Two sterol regulatory element-like sequences mediate up-regulation of caveolin gene transcription in response to low density lipoprotein free cholesterol. Proc Natl Acad Sci U S A. 1997; 94:10693–8. [PubMed: 9380697]

36. Baudino TA, McKay C, Pendeville-Samain H, Nilsson JA, Maclean KH, White EL, et al. c-Myc is essential for vasculogenesis and angiogenesis during development and tumor progression. Genes Dev. 2002; 16:2530–43. [PubMed: 12368264]

37. Mezquita P, Parghi SS, Brandvold KA, Ruddell A. Myc regulates VEGF production in B cells by stimulating initiation of VEGF mRNA translation. Oncogene. 2005; 24:889–901. [PubMed: 15580293]

38. Kang J, Rychahou PG, Ishola TA, Mourot JM, Evers BM, Chung DH. N-myc is a novel regulator of PI3K-mediated VEGF expression in neuroblastoma. Oncogene. 2008; 27:3999–4007. [PubMed: 18278068]

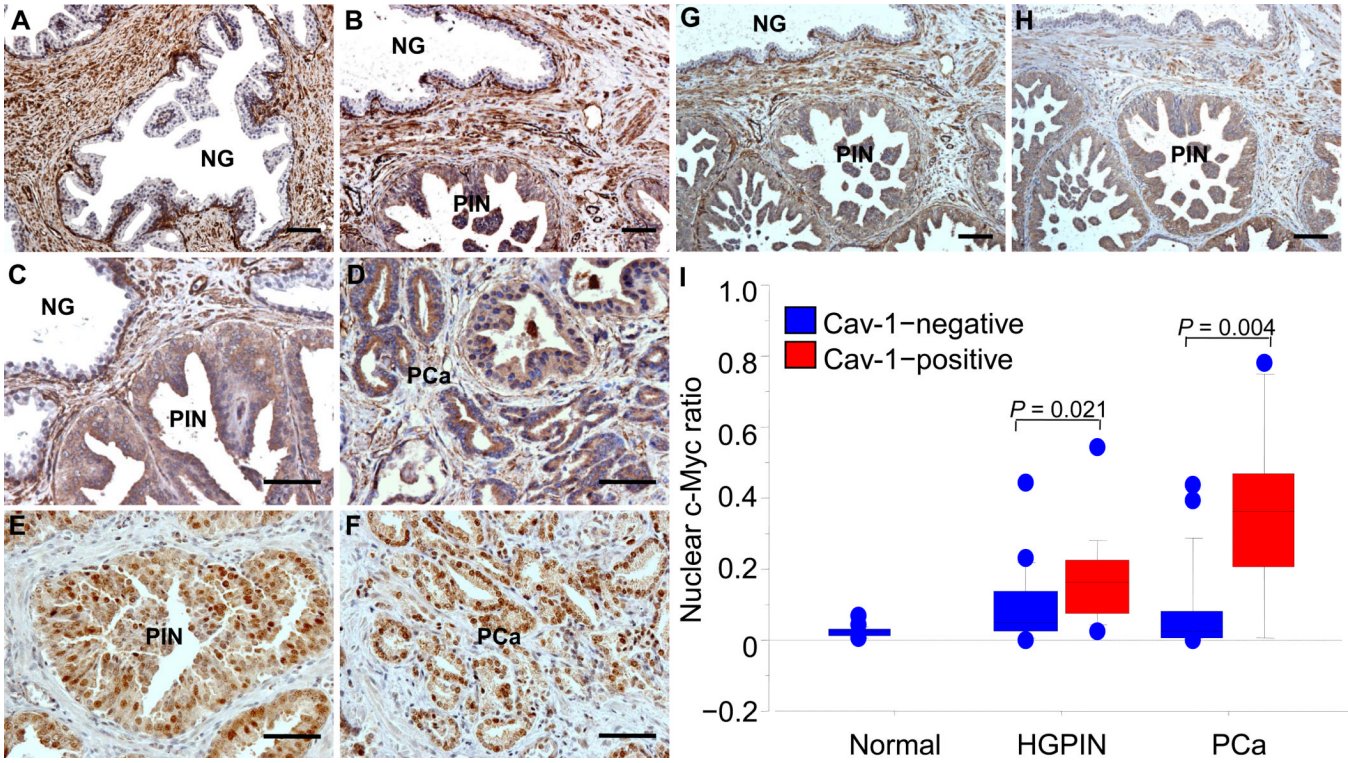

Figure 1.

Immunohistochemical staining shows Cav-1 (A through D) and c-Myc (E and F) expression in premalignant HGPIN or adenocarcinoma (PCa) of human prostate specimens from radical prostatectomies. A, in histologically normal prostate, Cav-1 was predominantly localized to stromal cells and some basal cells, whereas the luminal epithelial cells were negative for Cav-1 immunostaining (NG). B, Cav-1 was expressed in a HGPIN (PIN) lesion and, at higher power (C), it was observed in the cytoplasm of HGPIN cells but not in that of the normal luminal epithelia (NG) adjacent to the HGPIN. D, Cav-1 was also present in some cancer cells on the same slide as shown in (C). E and F, c-Myc immunostaining in HGPIN (E) and in PCa (F) in a prostate with Cav-1–positive HGPIN and PCa. HGPIN with positive Cav-1 staining(G) tended to show a high level of VEGF immunostaining (H), as demonstrated on these adjacent slides of the same specimen. Scale bars=100μm. I,box plots show results from quantitative analyses of nuclear c-Myc staining in normal luminal epithelia, HGPIN, and PCa cells of human prostates, as stratified by their Cav-1 immunostaining status. *P* values were derived by using Mann-Whitney rank testing. Each box indicates the values of middle 50% of data. The dark line within a box denotes the median, and the values between bars indicate the data ranging from the 10th to the 90th percentiles.

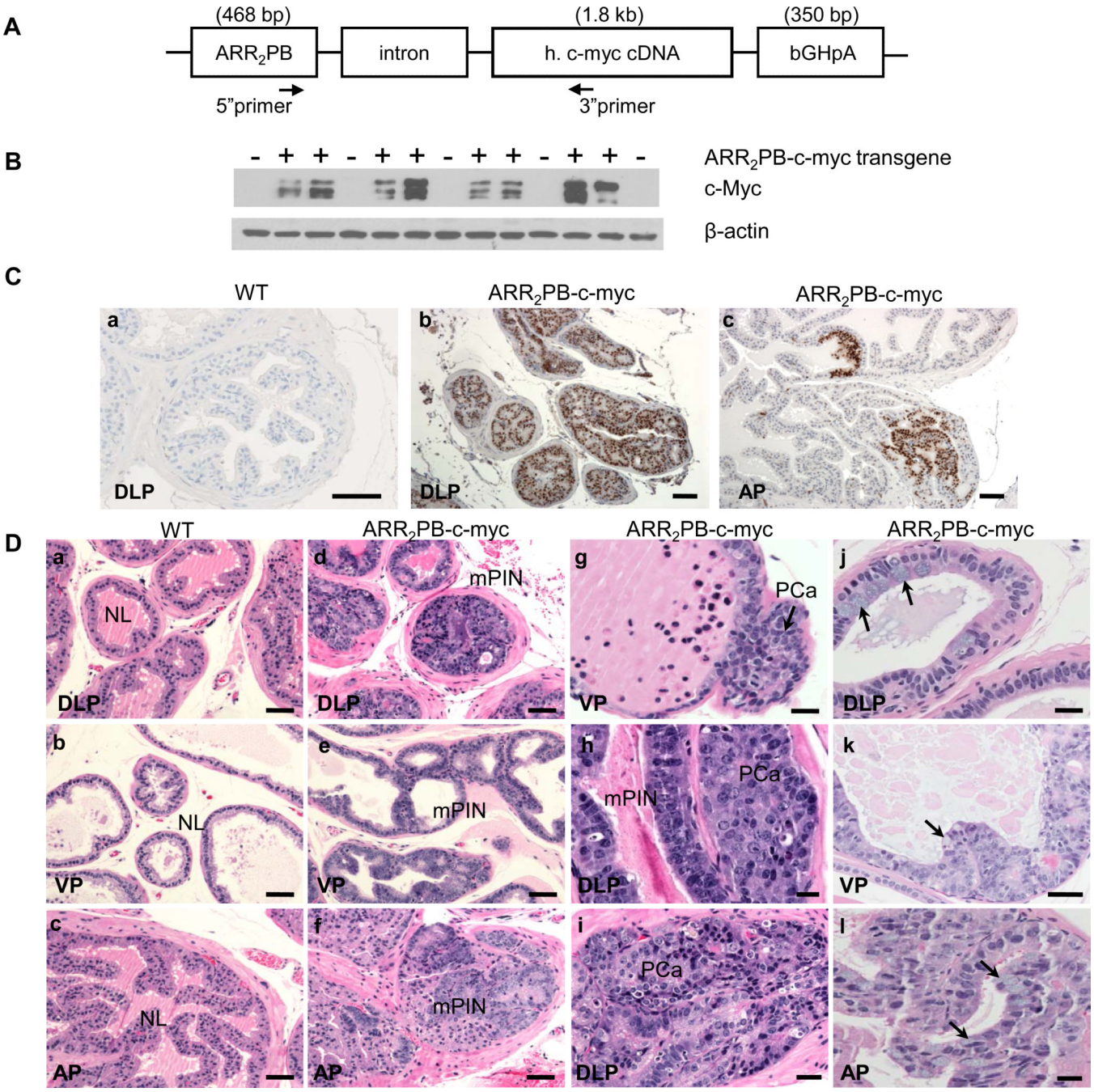

Figure 2.

Generation of ARR_2PB–c-myc transgenic mice and verification of expression of the c-Myc transgene. A, Schematic construction of the transgene. A 1.8-kb cDNA fragmentencoding human (h) c-Myc cDNA was cloned along with rabbit β-globin splice sequences (part of exon I, intron I, and exon II) and the bovine growth hormone polyA (bGHpA) site downstream of the rat PB promoter modified with two repeats of the ARR. Primers specific to the promoter and human c-Myc were used to confirm germline transmission of the transgene. B,ARR_2PB–c-myc transgene expression demonstrated by Western blotting. Total protein was extracted from the dorsolateral prostates of 6-month-old wild-type (n = 5, transgene-negative) and ARR_2PB–c-myc (n = 8, transgene-positive) mice; c-Myc expression

was determined by using a rabbit monoclonal c-Myc antibody, and β-actin was used as a loading control. C,immunohistochemical staining with a c-Myc–specific monoclonal antibody demonstrated expression of transgenic c-Myc in the prostates of 6-month-old mice. This antibody labeled the nuclei of neoplastic glandular epithelial cells in the transgenic (ARR_2PB–c-myc) prostate but not in the wild-type (WT) prostate. AP indicates anterior lobe; DLP, dorsolateral lobe; scale bars=100 μm. D, morphologic features of the prostates of WT (a through c) and ARR_2PB–c-myc transgenic (d through l) mice on hematoxylin- and eosin-stained sections. Extensive mouse prostatic intraepithelial neoplasia (mPIN) was present in the DLP and ventral (VP) lobes of the prostate of ARR_2PB–c-myc mice (d and e, respectively) but not in the normal WT prostates (NL, a through c). In the AP, mPIN tended to appear as focal lesions (f, arrows), which were not present in their WT counterparts (c). Microinvasive adenocarcinomas (PCa, g through i) were found adjacent to mPIN in both the VP (g, arrows) and DLP (h and i) lobes. Metaplasia of mucin-secreting cells (j through l, arrows) were found in the DLP (j), VP (k), and AP (l) lobes. Scale bars, b–f=60μm; a and g–l=30 μm.

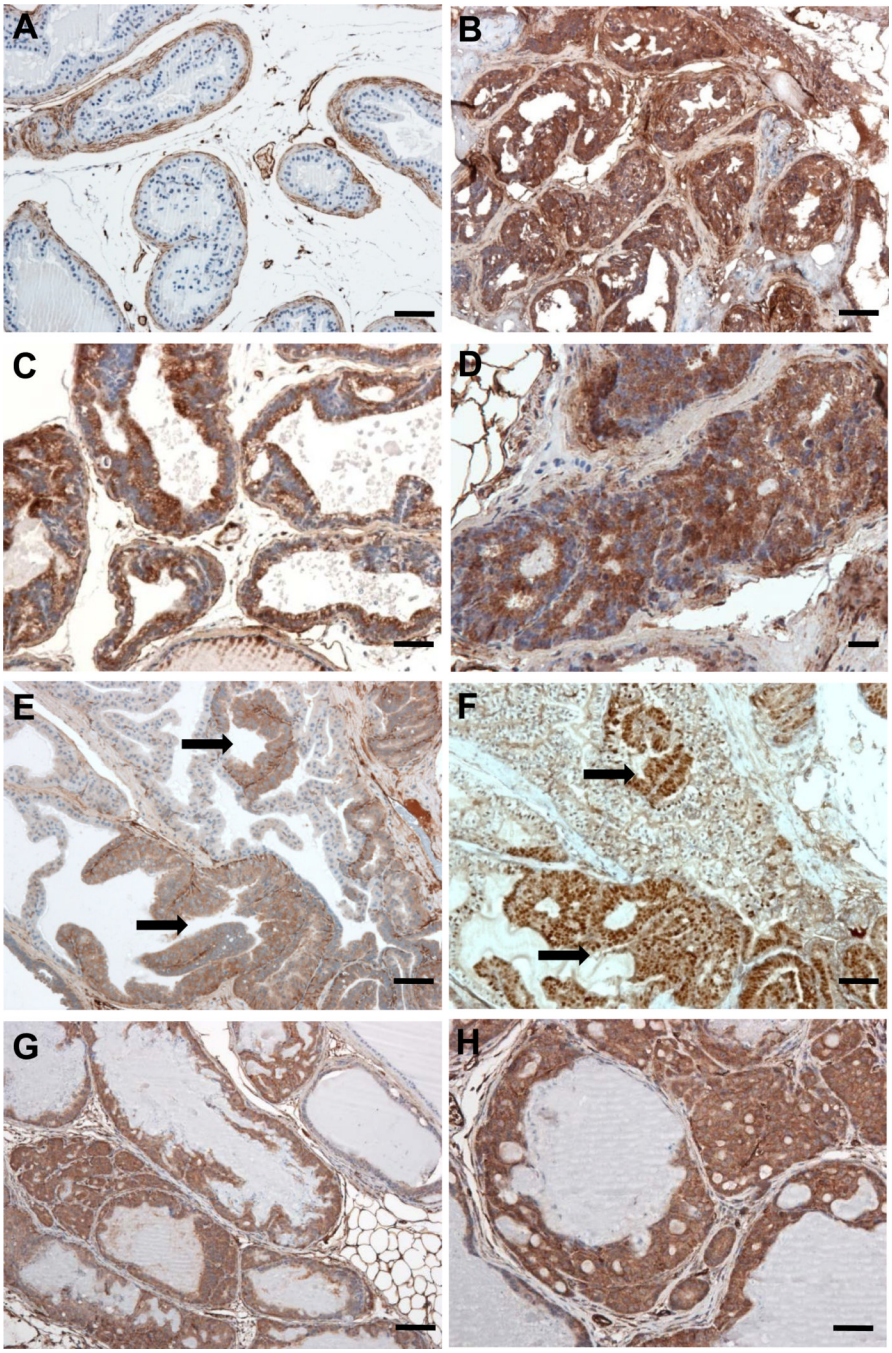

Figure 3.

Immunostaining shows Cav-1 overexpression in the prostates of ARR_2PB–c-myc mice. A, in the normal prostate of wild-type mice, Cav-1 was predominantly expressed in the stromal cells, including periglandular myofibroblasts and vascular cells, whereas the luminal epithelial cells were negative for Cav-1. Cav-1 was overexpressed in the mPIN lesions of the dorsolateral (B) and ventral (C) prostate lobes of 6-month-old ARR_2PB–c-myc mice. D, in the dorsolateral lobe of an ARR_2PB–c-myc mouse, Cav-1 was overexpressed in the adenocarcinoma invading into the prostatic stroma. In the anterior prostate lobe, Cav-1 overexpression in epithelial cells was confined to the mPIN lesion area (E, arrows) where the overexpression of human Myc was also demonstrated (F, arrows). In the Hi-Myc

transgenic model originally developed by Ellwood-Yenet al, Cav-1 was also highly expressed in the mPIN and adenocarcinoma lesions (G and H). Scale bars, A, B, and G=100 μm; C–F and H = 50 μm.

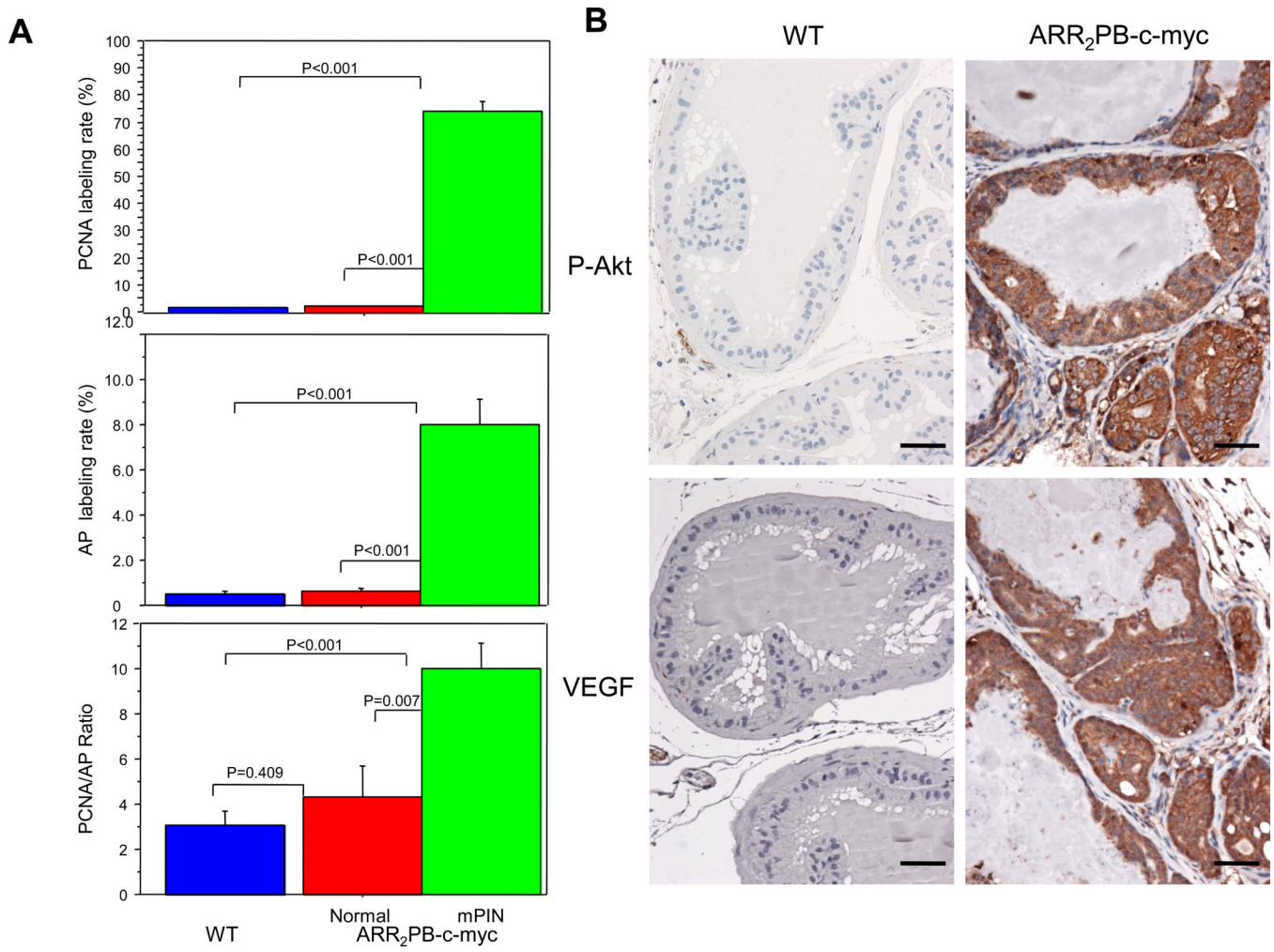

Figure 4.

A, quantitation of PCNA and apoptotic-body labeling by immunohistochemical staining and the TUNEL technique, respectively, in the anterior prostates of wild-type (WT; $n = 7$) and ARR_2PB–c-myc transgenic mice ($n = 7$). We compared the labeling rates of PCNA-positive cells (top panel) and apoptotic bodies (AP; middle) and the ratios of the labeling rates for PCNC and the apoptotic bodies (bottom) between the prostate epithelia of the WT mice, the normal epithelia adjacent to the mPIN lesions, and the mPIN lesions of ARR_2PB–c-myc mice. Data are expressed as means and standard error. *P* values were derived from ANOVA unpaired *t* testing. B,photomicrographs show that phospho-Akt (S473) and VEGF (bottom row) were overexpressed in the dorsolateral prostate of ARR_2PB–c-myc mice but not in those of the WT. Scale bars= 80 μm.

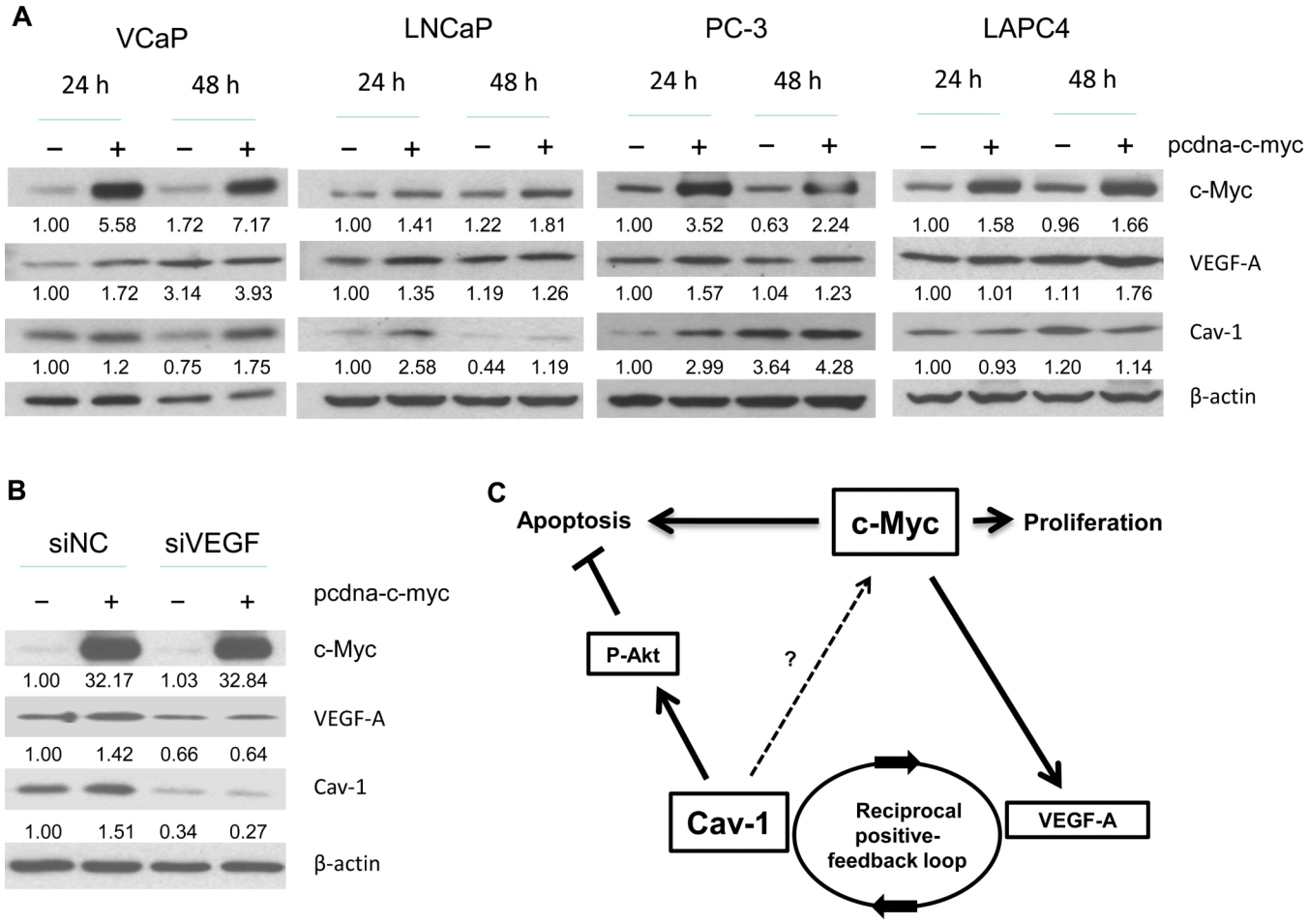

Figure 5.

Western blotting analysis showed that c-Myc induces Cav-1 expression in PCa cell lines. A, Cav-1 levels were increased in response to c-Myc in the PCa cell lines VCaP, LNCaP, and PC-3 but not in the LAPC4 line. Quantification of the relative levels of c-Myc, VEGF-A, and Cav-1 (the numbers under each band), normalized to the control β-actin level, are presented as the fraction of the control level at 24 hours. B, knockdown of VEGF-A by siRNA (siVEGF) transfection led to attenuation of the Cav-1 upregulation induced by c-Myc overexpression. PC-3 cells were transfected with non–target control siNC (30 nM) or VEGF-A–specific siRNA (30 nM) followed by transfection with pcdna3.1 vector or pcdna-c-myc. Results are for cell lysates collected 72 hours after VEGF-A siRNA transfection (48 hours after c-Myc transfection). Quantitative analysis of relative c-Myc, VEGF-A, and Cav-1 levels was done by normalizing the optical density of each band to that of the β-actin band within the same sample. The levels of c-Myc, VEGF, and Cav-1 were set as 1 for the siNC-negative control sample. **C**, Diagram illustrates potential interactions between c-Myc, Cav-1, VEGF-A, and P-Akt proteins in the development of prostatic intraepithelial neoplasia (PIN) and the transition to PCa. Cav-1 may mediate c-Myc–induced oncogenic activities by inhibiting apoptosis via P-Akt signaling. Upregulation of Cav-1 in PIN lesions may be due partly to an increased VEGF-A concentration resulting from c-Myc overexpression and the development of a positive-feedback loop.

Table 1

Correlative analyses of Cav-1 and c-Myc immunostaining in human prostate specimens

Cav-1 immunostaining: HGPIN vs prostate cancer					
		Prostate cancer			
		Cav-1 negative (*n*)	**Cav-1 positive (*n*)**	**Correlation coefficient**	***P***
HGPIN	Cav-1 negative (n = 21)	19	2	0.655	< 0.001
	Cav-1 positive (n = 15)	4	11		

c-Myc vs Cav-1 immunostaining in HGPIN and PCa					
		c-Myc negative (*n*)	**c-Myc positive (*n*)**	**Correlation coefficient**	***P***
HGPIN	Cav-1 negative (*n* = 17)	12	5	0.418	0.032
	Cav-1 positive (*n* = 14)	4	10		
PCa	Cav-1 negative (*n* = 19)	16	3	0.555	< 0.001
	Cav-1 positive (*n* = 12)	2	10		

Table 2

Histopathologic features and frequencies in the prostate of ARR_2PB-c-myc transgenic mice

Age (mo)	*n*	Wild-type	*n*	ARR_2PB-c-myc
3-4	2	2/2 normal	4	2/4 normal
				2/4 mPIN
6-8	12	11/12 normal	22	4/22 normal
		1/12 focal hyperplasia		18/22 mPIN
				2/22 microinvasive adenocarcinoma
				5/22 mucinous metaplasia
12-14	9	8/9 normal	9	8/9 mPIN
		1/9 focal hyperplasia		1/9 microinvasive adenocarcinoma
				4/9 mucinous metaplasia
≥ 15	3	3/3 normal	6	4/6 mPIN
				2/6 microinvasive adenocarcinoma
				2/6 mucinous metaplasia